# Effect of temperature on the wear behavior of NiTi shape memory alloy

Yan, Lina; Liu, Yong

2014

Yan, L., & Liu, Y. (2014). Effect of temperature on the wear behavior of NiTi shape memory alloy. Journal of materials research, 30(2), 186-196.

https://hdl.handle.net/10356/104737

https://doi.org/10.1557/jmr.2014.381

# Effect of temperature on the wear behavior of NiTi shape memory alloy

Lina Yan[a] and Yong Liu
*School of Mechanical and Aerospace Engineering, Nanyang Technological University, Singapore 639798*

(Received 19 July 2014; accepted 20 November 2014)

This article aims to provide a fundamental understanding of the deformation mechanisms of NiTi shape memory alloy (SMA) during the wear process at different temperatures when different microstructures are present. Three temperature regimes were selected namely, $T < M_f$, $A_s < T < A_f$, and $T > A_f$, where fully martensitic, martensite co-existing with austenite, and fully austenitic microstructures were formed, respectively. When $T < M_f$, it was observed that the coefficient of friction had decreased initially and thereafter stabilized at a lower value with increasing wear cycles. More decrease was found when the temperature was near to $A_s$. Furthermore, when tested above $A_f$, the coefficient of friction had decreased more significantly under higher load. Difference in the trend of coefficient of friction at different temperatures is originated from the different deformation mechanisms involved in the wear process, particularly the martensite detwinning process, the stress-induced phase transformation process, and the plastic deformation of martensite.

## I. INTRODUCTION

NiTi shape memory alloy (SMA) is an important candidate of advanced tribomaterial due to its superior wear resistance combined with good biocompatibility, corrosion resistance, superelasticity, one-way, and two-way shape memory effects.[1–5] Various studies have been performed on comparing the wear resistance of NiTi SMA with conventional wear resist materials. It has been reported that, for tests under different wear modes, both martensitic and austenitic NiTi SMAs showed better wear resistance than that of the conventional wear resist materials such as AISI 304 stainless steel, GCr15 steel, BS11 rail steel, 2024 aluminum, Co45 alloy, and surface nitride 38 CrMoAIA alloys.[6–11] The good wear resistance in martensitic NiTi SMA has been attributed to the deformation strain accommodation through a detwinning process, which is accompanied by a stress-plateau on the stress–strain curve.[6–8] While the good wear resistance in austenitic NiTi SMA has been attributed to the deformation strain accommodation through a stress-induced martensitic transformation (SIMT) process, which is accompanied by a pseudoelastic stress–strain curve.[11,12] In addition, the concept of phase-transformational shakedown due to the canceling out of transformation strain has been suggested in further contributing to the wear resistance of NiTi SMA.[13]

Furthermore, studies have compared the wear resistance of austenitic and martensitic NiTi SMAs, and the austenitic NiTi SMA has been reported to possess even better wear resistance.[12,13] Therefore, the pseudoelasticity (also known as superelasticity) of austenite has been suggested as the more effective contributing factor in resisting wear. Nevertheless, it was also noted that when tested under high magnitude of load, NiTi SMA possessing different levels of pseudoelasticity behaved similarly in the wear process.[14] This has been attributed to the large deformation occurred under high load, which weakened the effectiveness of pseudoelasticity in accommodating the deformation strain. Therefore, different wear mechanisms that might be activated under high load resulted in different wear behavior in the NiTi SMA.[14,15]

It is known that, different from conventional structural materials, SMA experiences thermo-elastic phase transformations and its microstructure is sensitive to the temperature change.[2] Since the deformation mechanism during the wear process is sensitive to the microstructural state (martensitic or austenitic), it is of ultimate importance to understand the effect of temperature on the wear behavior of NiTi SMA to use it effectively. However, the deformation mechanisms that were activated under different contact stresses due to different magnitudes of applied loads have rarely been discussed in the previous wear studies. In the present research, we have systematically investigated the effect of temperature on the wear behavior of NiTi SMA under different applied loads. This study has focused on the deformation mechanisms during the wear process, and the accumulation of surface damage was related to the plastic strain accumulation during repeated wear cycles. The microscale wear tests were conducted and the tests were stopped once severe damage occurred on the surface. The wear behavior has been

[a]Address all correspondence to this author.
e-mail: linayan@ntu.edu.sg
DOI: 10.1557/jmr.2014.381

  

analyzed based on the observations of the coefficient of friction and the corresponding surface wear features as a function of temperature, load, and wear cycles. The microstructural responses of the NiTi SMA at different temperatures and under different loads were discussed through taking into consideration the phase transformation temperatures and the estimated contact stresses, and the corresponding deformation mechanisms in the wear process were proposed.

## II. EXPERIMENTAL

Transformation temperatures of a forged ingot of Ni–Ti SMA used in the present research were determined using a TA Instruments Q200 differential scanning calorimeter (DSC). The heating rate was 2 °C $min^{-1}$ and several thermal cycles were repeated to verify the results. The martensitic starting ($M_s$) and finishing ($M_f$) temperatures were 56 and 36 °C, while the austenitic starting ($A_s$) and finishing ($A_f$) temperatures were 66 and 92 °C, respectively. To investigate the wear behavior using the tribometer with a CETR UMT multispecimen system, specimens with a dimension of 10 mm × 10 mm × 1 mm were prepared. The samples were mounted onto an acrylic resin substrate for ease of handling. In the sample preparation process, the surface was mechanically grinded and polished, thus the preexisted surface oxide layer was removed. The samples were then held at 150 °C for 10 min to release the residual strain. According to Firstov et al.,[16] near-zero oxidation occurred on a bare NiTi surface when heat treatment was conducted at temperatures below 300 °C. Hence, the effect of surface oxide on the wear behavior of NiTi SMA is ignorable in this study. Thereafter, the sample surfaces were characterized by a DI3000 atomic force microscope (AFM) in tapping mode. During surface characterization, three different areas of 10 × 10 $\mu m^2$ arbitrarily selected were scanned. Only specimens with average surface roughness (Ra) value below 15 nm were used in the subsequent wear tests. Ball-on-disk sliding wear tests were conducted, and the alumina counter-ball with a diameter of 4 mm was used. Specimens were tested at 20, 90, and 120 °C under applied loads ranged from 50 to 300 mN, respectively. The sliding speed was at 4.71 mm $s^{-1}$ and the sliding distance was estimated to be 9420 mm for 1000 wear cycles. Moreover, once the force detected had reached the acceptable level, the test was stopped to protect the cantilever. After each wear test, the surface wear features were examined using a laser confocal microscope (Nikon Eclipse L150). The profiles of wear features (width of tracks) were quantitatively measured by using the confocal imaging system. Due to the small scale wear test, the direct measurement on the material loss was not applicable, and partial of tests has resulted in insignificant damage, which was even not visible.

The testing temperature was determined by a thermal couple that in direct contact with the specimen before running the wear test. However, the local temperature rise was likely involved in the wear process, especially on the tip of contact. The instant temperature variation was unknown since no method of precise measurement has been developed. In this study, a small-scale wear test was specially chosen (counter-ball with a diameter of only 4 mm) with low-sliding speed to minimize the local temperature rise at a contact tip.

## III. RESULTS

At different temperatures, NiTi SMA possesses different microstructures, which result in different deformation mechanisms in the wear process. To systematically reveal the effect of temperature on the wear behavior of NiTi SMA, the coefficient of friction and the corresponding surface wear features were studied as a function of temperature and load. In the present study, tests were stopped when severe damage occurred on the surface, hence a minimal material loss was involved. Surface wear features were imaged after each test and the width of wearing tracks was quantitatively measured for wear estimation. On the other hand, the coefficient of friction is a direct measurement of frictional force, which is closely related to the amount of damage/debris formed on surface after repeated wear cycling.[17] When the frictional force is extremely low, the coefficient of friction is also extremely low and no permanent damage occurs on surface. However, with increasing frictional force, more damage will be induced during the wear test, hence coefficient of friction will be increased.

In the following, the wear results obtained at different temperatures consisting of different initial microstructures will be explained and the corresponding surface features will be presented.

### A. Effect of temperature and load on the coefficient of friction

#### 1. Wear behavior at 20 °C

When tested at 20 °C, the NiTi SMA specimen was in the martensitic state. When the contact stress approaches stress-plateau, the martensite detwinning process starts and the deformation is recoverable only when heated above $A_f$ temperature. Deformation strain can be accommodated through such a detwinning process, which will reduce the plastic strain, hence reduce the wear. As shown in Figs. 1(a)–1(d), under different applied loads, the coefficients of friction as a function of wear cycles behaved differently.

Under 50 mN [Fig. 1(a)], the coefficient of friction had increased to around 0.37 after 100 wear cycles. It scattered around this value in the remainder of test and

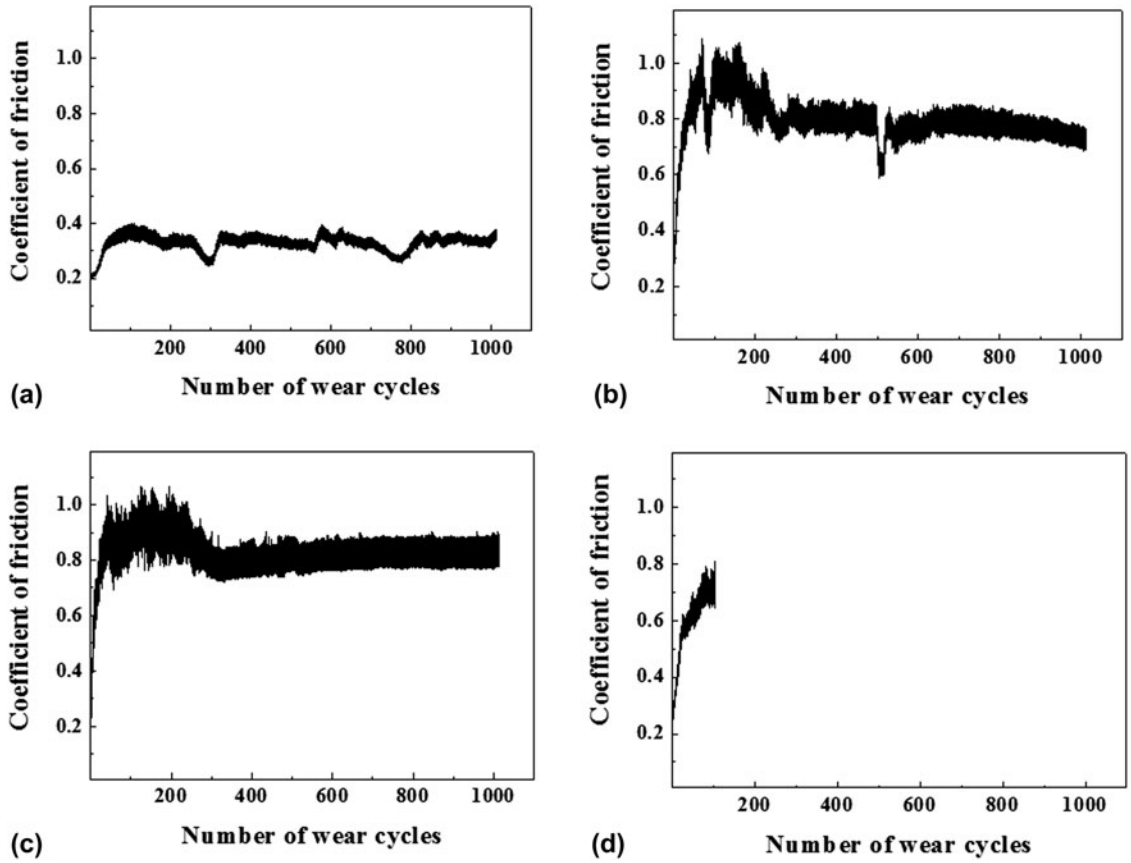


FIG. 1. The coefficients of friction as a function of wear cycles when tested at 20 °C under several applied loads: (a) 50 mN, (b) 100 mN, (c) 200 mN, and (d) 300 mN, respectively.

a maximum/minimum value of around 0.4/0.25 was observed. However, when the load was increased to 100 mN, the coefficient of friction had reached to around 1.0 after about 100 wear cycles [Fig. 1(b)]. More interestingly, the coefficient of friction decreased to around 0.8 from 280 wear cycles onward and remained around this value throughout the test. From 50 to 100 mN, different deformation mechanisms likely have been activated at increased load, which will be further discussed in this article. The load was further increased to 200 mN [Fig. 1(c)], and the coefficient of friction showed a similar trend to that under 100 mN. It had increased to around 1.0 after 100 wear cycles and started to decrease thereafter. A stabilized value of around 0.8 was reached after about 300 wear cycles and it was maintained in the remainder of test. The clear decrease in the coefficient of friction followed by a stabilization behavior was observed when the load was at 100 and 200 mN. Under these loads, a similar deformation mechanism has dominated the wear process, leading to similar trends in coefficients of friction. When a load of 300 mN was applied [Fig. 1(d)], the coefficient of friction was highly unstable and the test was stopped after around 100 wear cycles. Under 300 mN, the NiTi SMA surface had degraded more significantly in a short period due to extremely high contact stress.

## 2. Wear behavior at 90 ˚C

When the temperature was increased to 90 °C ($A_f$ is at 92 °C), partial of martensite transformed into austenite. Due to the SIMT of the co-existing austenitic phase, at 90 °C, the dominating deformation mechanism is expected to be different from that at 20 °C, hence resulting in different wear behavior.

As shown in Fig. 2(a), under a load of 50 mN, the coefficient of friction had increased to around 0.4 after about 150 wear cycles and remained at around an average value of 0.35 till the end of the test. During the repeat tests, we have also observed some sudden increase in the coefficient of friction followed by a quick return to the stable range. Since the signal was extremely low, we believe that the sudden increase in the coefficient of friction was likely caused by the background noise. Under 100 mN [Fig. 2(b)], the coefficient of friction had reached to around 0.9 after about 50 wear cycles [Fig. 2(b)]. Starting from around 250 wear cycles, it decreased and then stabilized at around 0.38. Such

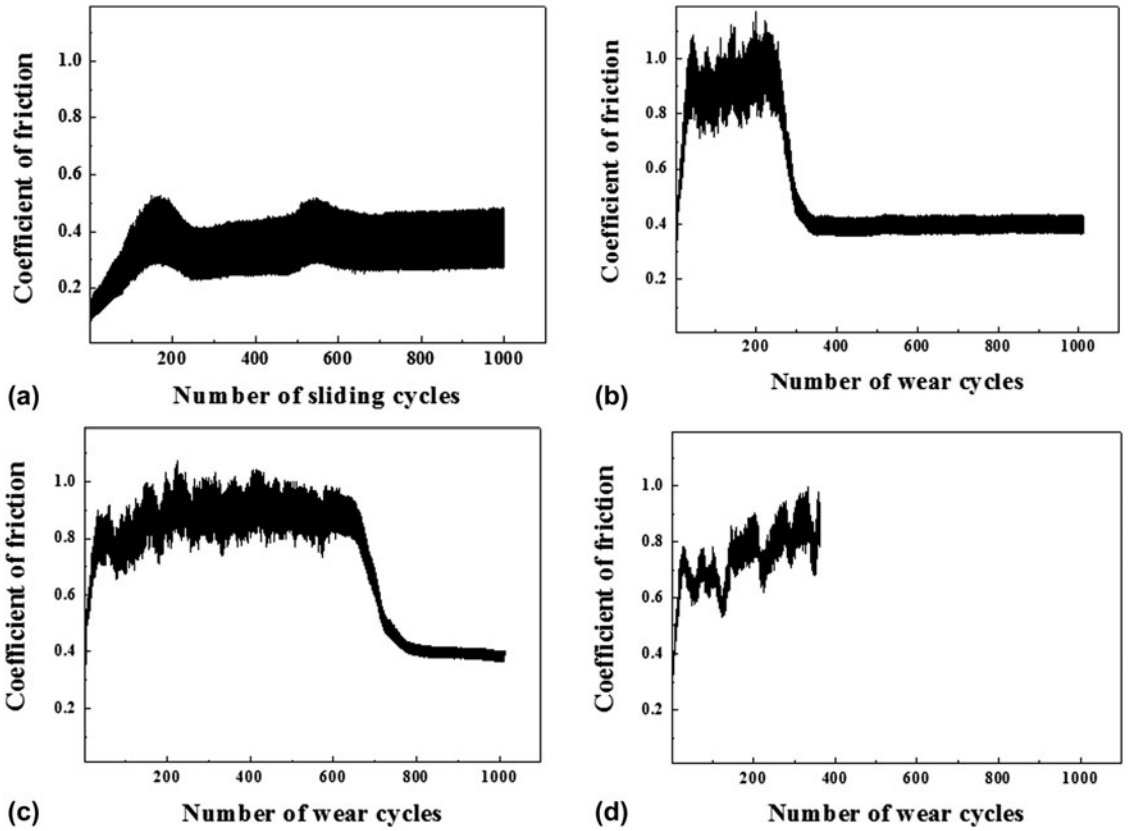


FIG. 2. The coefficients of friction as a function of wear cycles when tested at 90 °C under several applied loads: (a) 50 mN, (b) 100 mN, (c) 200 mN, and (d) 300 mN, respectively.

a behavior in coefficient of friction has never been reported in the literature. It is worth noting that tested at 20 °C, the coefficient of friction of the fully martensitic NiTi had decreased from around 1.0 to 0.8 under 100 and 200 mN [Figs. 1(b) and 1(c)]. Therefore, at 90 °C, the large drop in the coefficient of friction from around 0.9 to 0.38 is likely associated with SIMT of an austenite phase in the sample.

When under 200 mN, the coefficient of friction had reached around 0.9 after about 200 wear cycles [Fig. 2(c)]. After approximately 680 wear cycles, it started to decrease and finally stabilized at around 0.4 from 800 wear cycles onward. Under 100 and 200 mN, it is envisaged that similar deformation mechanism was involved. The coefficient of friction had dropped by nearly 50%, which is much higher than the decrease that has been reported by Qian et al.[6,13] Furthermore, the reported decrease in the coefficient of friction proceeded gradually and the stabilization process started after approximately 10,000 wear cycles. When under a load of 300 mN, the coefficient of friction was highly unstable and therefore, the test was stopped at around 400 wear cycles [Fig. 2(d)]. High instability in the coefficient of friction under 300 mN indicated significant damage caused by high contact stress.

## 3. Wear behavior at 120 ˚C

When the temperature was further increased to 120 °C, which was much higher than the $A_f$ temperature, the martensite phase was fully transformed into austenite. The fully austenitic NiTi experiences SIMT under load, which can be fully reversible. At 120 °C, the coefficients of friction as a function of wear cycles under several applied loads are presented in Figs. 3(a)–3(d).

Under 50 mN [Fig. 3(a)], the coefficient of friction had reached as high as 0.65 after approximately 100 wear cycles. After about 150 wear cycles, it started to decrease and then stabilized at an average value of around 0.4 till the end of test (scattered between 0.3 and 0.53). Under 100 mN, the coefficient of friction had increased to about 0.42 after approximately 20 wear cycles and decreased slightly with further increasing wear cycles [Fig. 3(b)]. After 100 cycles, it stabilized at around 0.3 and maintained this value in the remainder of test. The smaller scattering in the coefficient of friction observed under 100 mN than that under 50 mN was unexpected. The large scattering under 50 mN was likely due to the background noise when the signal was extremely low, and this observation was consistent with that tested at 90 °C under 50 mN. As compared with the results obtained at 20 and 90 °C, the rather low

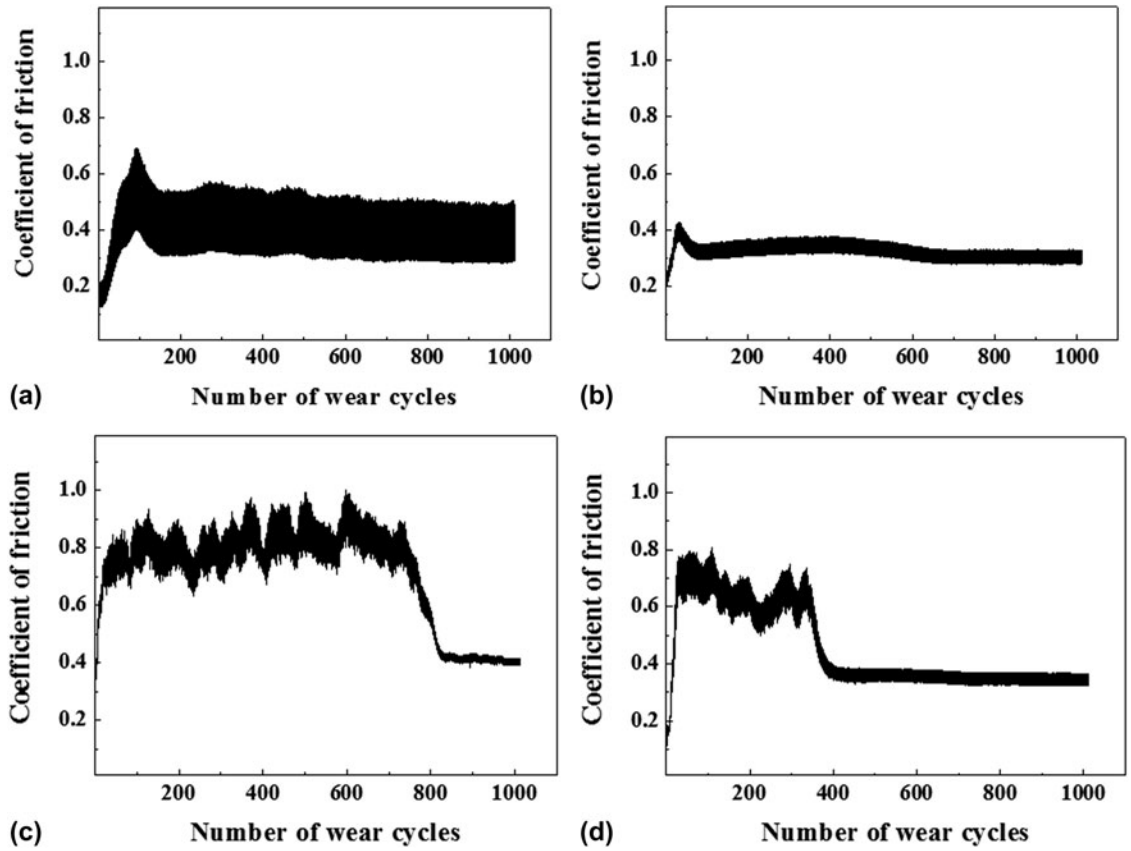


FIG. 3. The coefficients of friction as a function of wear cycles when tested at 120 °C under several applied loads: (a) 50 mN, (b) 100 mN, (c) 200 mN, and (d) 300 mN, respectively.

coefficients of friction at 120 °C are due to the reversible SIMT process.

The decrease-and-stabilization behavior of the coefficient of friction was also observed when under a load of 200 mN. The coefficient of friction had increased to around 0.8 after 50 wear cycles and it was maintained around this value for up to 700 wear cycles [Fig. 3(c)]. Thereafter, it decreased and restabilized at around 0.4 starting from around 820 wear cycles till the end of test. Under 300 mN, the coefficient of friction had reached to around 0.7 after 50 wear cycles [Fig. 3(d)]. After around 350 cycles, the coefficient of friction decreased and stabilized at 0.35 throughout the remainder of test. Different from other tests at lower temperatures, no instability in the test was encountered, suggesting less surface damage at 120 °C. This observation is consistent with the recoverable deformation mechanism of the austenite phase. The large decrease in the coefficient of friction occurred only when tested at 90 and 120 °C, where the austenite phase was presented further confirming the role of austenite in resisting wear.

All the tests were repeated for three times, although the curves of coefficients of friction did not exactly overlay with each other, the trends were similar. The increase in the coefficient of friction at the early stage of the test likely belongs to the run-in period in which surfaces adapted to each other through plastic deformation of high asperities.[18,19]

The coefficient of friction at 100th (run-in stage) and 1000th (stable stage) testing cycles was plotted as a function of temperature and load in Figs. 4(a) and 4(b). For 100 wear cycles, the temperature showed an insignificant effect on the coefficient of friction under different magnitudes of load, particularly 200 and 300 mN loads [Fig. 4(a)]. However, for 1000 wear cycles, the stabilized coefficient of friction was in a clearly decreasing trend as a function of temperature for loads of 100 and 200 mN [Fig. 4(b)]. Under 50 mN, the coefficient of friction was nearly unchanged with increasing temperature. In this case, the dominating deformation mechanism was likely not affected by the microstructures, which might be due to extremely low load. The coefficients of friction under 300 mN are not plotted in Fig. 4(b) since tests were stopped before 1000 wear cycles were reached due to high instability in some wear tests described previously.

## B. Surface wear features

After each test corresponding to Figs. 1–3, the surface wear features had been imaged to reveal the wear mechanism as well as to estimate the wear loss. After tested at

20 °C under 50 mN, asperities embossed on the surface were observed as shown in Fig. 5(a). The special surface wear feature has been named as "crown-like structure" in our previous report.[20] In addition, after tested at 20 °C under 100 mN and above, the deep tracks and increased amount of debris were observed [Figs. 5(b)–5(d)]. At 90 °C, a similar "crown-like structure" had been observed under 50 mN, and the tracks and debris were present when the load was further increased. At 120 °C, the "crown-like structure" was also observed under 50 and 100 mN. This observation confirmed insignificant wear occurred on surface and was in consistent with the low coefficient of friction as shown in Fig. 4. On increasing the load to 200 and 300 mN, tracks and debris were observed.

To further analyze the wear behavior, the widths of track were plotted as a function of temperature as shown in Fig. 5(e). The values were obtained by averaging 10 readings at different locations on the confocal image. Tested at 120 °C under several loads, the width of track after 1000 wear cycles was lower than that at 20 and 90 °C. This result is consistent with the lower value of stabilized coefficient of friction at 120 °C. On the other hand, with increasing load, more surface damage was caused thus the width of track was increased accordingly.

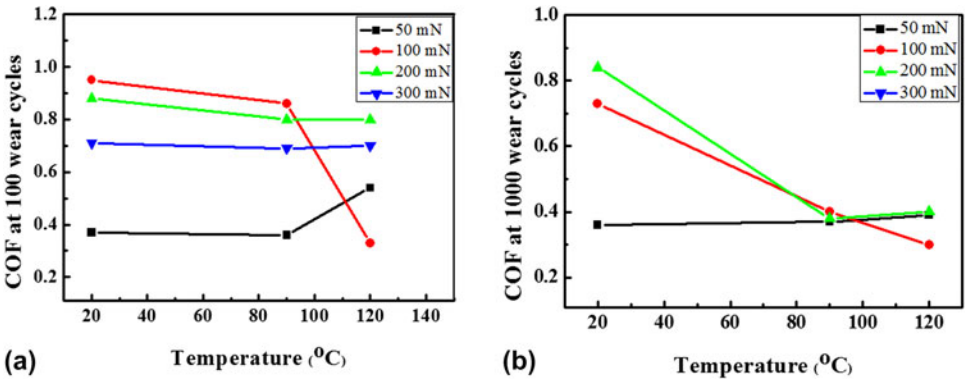


FIG. 4. The coefficient of friction as a function of temperature at (a) 100th testing cycle and (b) 1000th testing cycle.

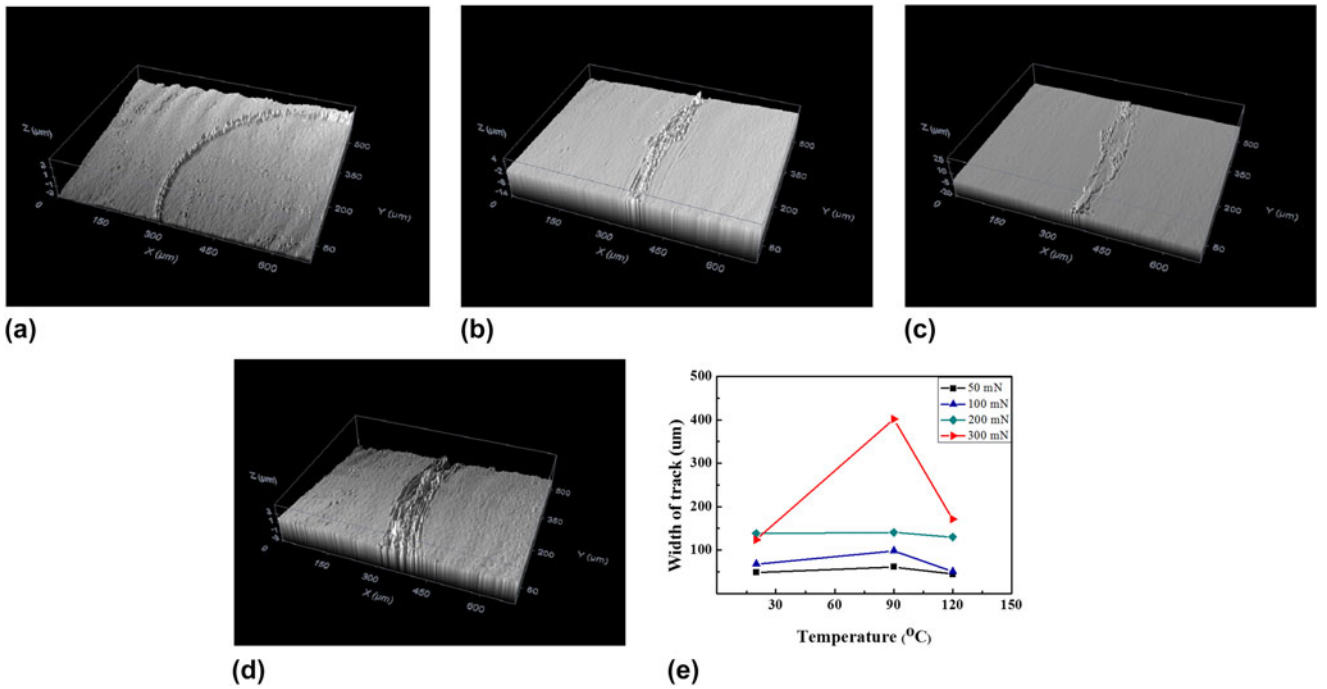


FIG. 5. 3D confocal microscopic image of the worn surface tested at 20 °C, (a) under 50 mN; (b) under 100 mN; (c) under 200 mN; (d) under 300 mN; and (e) the average width of track as a function of temperature.

### C. Summary of the results and classification of the wear stages

In the present study, instead of direct measurement on the material loss, we have used the width of tracks to estimate the wear. Meanwhile, the coefficients of friction as a function of wear cycle were used to compare wear resistance of surfaces. According to the observations in the coefficients of friction and surface wear features, the wear behavior of the NiTi SMA can be classified into three different stages. Stage I is a near-zero wear stage which is characterized by insignificant surface damage even after a large number of wear cycles accompanying by a low coefficient of friction. One example of such wear stage is shown in Figs. 1(a) and 5(a). At 20 °C under 50 mN, the coefficient of friction was very low and a crown-like structure had been formed after 1000 wear cycles. Similar wear behavior was also observed when tested at 90 and 120 °C under 50 or 100 mN. Stage II is a transition wear stage which is characterized by deep tracks and large amount of debris, as well as high coefficient of friction. During this stage, the coefficient of friction had shown a transition behavior with increasing wear cycles, and such transitions are usually correlated with changes in the deformation mechanisms. With increasing temperatures, the coefficient of friction had decreased significantly after transition, hence the accumulation of damage on the surface was reduced in further wear cycling. Examples of such behavior are shown in Figs. 1(b) and 2(b). The magnitude of the decrease in the coefficient of friction was dependent on the microstructure of NiTi SMA which is sensitive to the temperature. Therefore, the change in the deformation mechanism during a transition wear stage is closely related to the microstructure of NiTi SMA, which will be discussed further. Stage III is an abrasive wear stage which is characterized by severe surface damage as well as high instability in coefficient of friction. For example, when tested at 20 and 90 °C under 300 mN [Figs. 1(d) and 2(d)], the coefficients of friction were highly unstable, meanwhile, the widths of the wear tracks [Fig. 5(e)] were extremely high.

## IV. DISCUSSION

To understand the wear behavior of NiTi at different temperatures, the present discussion will focus on the deformation mechanism that is likely activated at different temperatures when different microstructures are present. These microstructures include (1) fully martensitic at $T < M_f$, (2) fully austenitic at $T > A_f$, and (3) martensite coexisted with austenite at $M_f < T < A_f$.

### A. Wear behavior at 20 °C ($T < M_f$)

At 20 °C, the NiTi SMA specimen is in martensitic state. It is known that the deformation of martensitic NiTi SMA proceeds in the following sequence: (1) elastic deformation of twinned martensite, (2) detwinning of twinned martensite with the occurrence of stress-plateau in the stress–strain curve, (3) elastic deformation of detwinned martensite, and (4) plastic deformation of detwinned martensite.[18,19] Since part of the initial deformation strain can be accommodated through a detwinning process by the formation of detwinned martensite, plastic deformation can be retarded. Hence, the good wear resistance in martensitic NiTi SMA has been attributed to the detwinning process which reduces plastic strain accumulation in repeated wear (sliding) cycles. On the other hand, the deformation mechanism involved in the wearing process is also related to the stress distribution in the contact area, which is nonuniform as indicated in the ball-on-disk contact model previously.[19] The highest contact stress occurs in the contact area that is closest to the tip of the counter-ball at which the deformation is the largest. Hence, the deformation mechanism in this area dominates the surface wear process and will be paid particular attention when explaining the wear mechanisms involved at different testing temperatures.

At 20 °C when the applied load is low, the contact stress is below the critical stress for detwinning, and the martensitic NiTi SMA behaves elastically. Therefore, the wear will be insignificant due to the insignificant plastic strain accumulation. For example, when tested under 50 mN, the coefficient of friction was maintained at a low value while asperities were embossed on the surface [Figs. 1(a) and 5(a)]. Since the formation of asperities had an insignificant effect on the coefficient of friction, the wear was in the near-zero wear stage. Insignificant wear occurred under 50 mN even after 1000 wear cycling, hence the overall contact stress was likely below the stress-plateau and the elastic deformation of twinned martensite had dominated the contact area. The Hertzian contact model was used to estimate the contact stress and the following equations were applied:[21,22]

$$\sigma^3 = \left[6F_n(E^*)^2\right] \Big/ \left(\pi^3 R^2\right) \quad , \tag{1}$$

$$1/E^* = \left(1-\nu_1^2\right)/E_1 + \left(1-\nu_2^2\right)/E_2 \quad , \tag{2}$$

where $\sigma$ is the contact stress, $F_n$ is the applied load, $R$ is the radius of the sphere (2 mm), $E_1$ and $E_2$ are the elastic moduli of the martensitic NiTi and the alumina ball, having values of 26 and 375 GPa, respectively. In addition, $\nu_1$ and $\nu_2$ are the Poisson's ratio for the martensitic NiTi and the alumina ball with values of 0.33 and 0.23. Therefore, by using Eqs. (1) and (2), the estimated contact stress under 50 mN was at 122 MPa. From the tensile stress–strain measurement at 20 °C, the stress-plateau of the martensitic NiTi was at 157 MPa,

which was comparable to those reported.[22] Therefore, this calculation has supported the assumption that the contact stress under 50 mN load was below the martensite stress-plateau, and elastic deformation had dominated the wear process.

With increasing load hence increasing the contact stress to reach the stress-plateau, detwinning of martensite occurs. Such a type of deformation is reversible when the specimen is heated to above $A_f$. To understand the active deformation mechanisms, the contact stress was also estimated. Similar to the previous calculation, by using the Hertzian contact model [Eq. (1)], the contact stress under 100 mN was estimated at around 153 MPa which is very close to the experimentally determined critical stress for detwinning (i.e., 157 MPa at 20 °C). Therefore, under 100 mN, the detwinning process had likely dominated the contact area. Under repeated wear cycles, more twinned martensite will become detwinned and plastic strain can be accumulated due to an irreversible process of detwinning at constant temperature. Examples are shown in Figs. 1(b) and 1(c) in which the wear behavior is similar when tested under 100 and 200 mN. The coefficient of friction had decreased from around 1.0 to 0.8 and stabilized thereafter, while tracks and debris had been formed after 1000 wear cycles due to plastic strain accumulation.

It is worth to note that the Hertzian contact model is only suitable for elastic deformation and the calculated contact stress will have large discrepancy with the true value if nonelastic deformation occurred. Therefore, the Hertzian contact model is not applicable for the contact stress calculation under 200 mN, since the contact stress has exceeded the critical stress for detwinning and the transition wear was occurred. Nevertheless, under high load, when the contact stress exceeds the yield stress of detwinned martensite, plastic deformation is the predominant mechanism in the contact area. Debris can be generated in the beginning of the test and severe wear occurs after a few wear cycles. This can explain the observations under 300 mN [Figs. 1(d) and 5(d)] in which tracks and debris were formed when tested for even less than 100 wear cycles. High instability in the coefficient of friction was observed and severe damage was found on the surface, and the wear was in the abrasive wear stage. In this case, plastic deformation of detwinned martensite had dominated the contact area.

### B. Wear behavior at 120 °C ($T > A_f$)

When the temperature is increased to above $A_f$ but below $M_d$ (the highest temperature for SIMT), the deformation of austenitic NiTi SMA will proceed in the following sequence: (1) elastic deformation of austenite, (2) SIMT with the occurrence of stress-plateau in the stress–strain curve, (3) elastic deformation of stress-induced martensite, and (4) plastic deformation of stress-induced martensite.[23,24] During deformation of austenite, a deformation strain up to about 10% can be fully accommodated through the SIMT process which can be fully recoverable upon unloading. Due to the pseudoelasticity of austenite, plastic deformation can be effectively reduced and the plastic strain accumulation in the repeated wearing cycles can be insignificant when the deformation strain keeps within this range. Therefore, the superior wear resistance of austenitic NiTi SMA has been attributed to the pseudoelasticity. The stress-plateau for SIMT at 90 °C was at around 320–370 MPa as obtained from tensile tests. According to the Clausius–Clapeyron equation, the critical stress for SIMT increases with increasing temperatures.[25] McKelvey and Ritchie[26] have studied the effect of temperature on the critical stress at plateau, and the Clausius–Clapeyron equation has been modified to give:

$$\mathrm{d}\left(\sigma^T\right)/\mathrm{d}T = -\Delta h \rho_A / T\varepsilon_0 \quad , \tag{3}$$

$$\sigma^T - \sigma^0 = \left(-\Delta h \rho_A\right)/\varepsilon^T \ln(T/T_0) \quad , \tag{4}$$

where $\sigma$ is the applied stress and $\varepsilon_0$ is the amount of strain due to SIMT. Since the enthalpy has been measured via the DSC tests and was in terms of energy/mass ($\Delta h$), it was multiplied by the density of austenitic NiTi ($\rho_A$ = 6.45 g cm$^{-3}$) to maintain consistency of units. In addition, the $T$ is in the unit of K. Therefore, the critical stress at 120 °C was calculated at around 528 MPa with reference to around 320 MPa at 90 °C. The critical stress for SIMT at 120 °C is below the critical stress for dislocation generation which has been reported at around 750–900 MPa, hence the austenitic NiTi SMA behaves pseudoelastically.[26]

At 120 °C, when the contact stress is below the critical stress for inducing martensitic transformation, elastic deformation of austenite dominates the contact area, causing insignificant wear on surface. Furthermore, the critical stress increases with increasing temperature, which allows more deformation strain accommodating under higher loads. Therefore, the near-zero wear stage is prolonged, hence the wear resistance of NiTi is improved at increased temperature.

One example is the wear tests under 50 and 100 mN, where low coefficients of friction as well as crown-like structures had been observed [Figs. 3(a) and 3(b)]. By using the Hertzian contact model with Young's modulus of austenitic NiTi around 75 GPa, the calculated contact stress was at around 230 and 290 MPa for 50 and 100 mN loads, respectively. Both values were much lower than the critical stress (528 MPa at 120 °C) for SIMT, hence the elastic deformation of an austenite phase is the dominating mechanism involved in the wear tests.

This further explains the very low coefficient of friction and its stability during the wear tests.

Further increasing contact stress, SIMT and elastic deformation of stress-induced martensite will occur. Under even higher load where the contact stress exceeds the yield stress of stress-induced martensite, plastic deformation will dominate the contact area. However, due to effective deformation strain accommodation through the reversible SIMT process, the plastic deformation can be retarded, which contributed to the wear resistance of austenitic NiTi SMA.

For tests under 200 and 300 mN, the coefficients of friction decreased from around 0.8 to 0.4, while certain damage was found on surfaces. Less wear occurred in the stabilized wearing process and lower coefficient of friction was observed. The mechanism had transited from initial plastic deformation dominated by adaption of high asperities to the pseudoelastic deformation responsible for the stabilized wear process. Therefore, at 120 °C, the wear resistance of the NiTi surface was effectively improved by the deformation strain accommodation through a SIMT process as compared with that at 20 °C.

### C. Wear behavior at 90 °C ($M_f < T < A_f$)

When the temperature is above $M_f$ but below $A_f$, the twinned martensite will co-exist with the austenite. In general, when two phases co-exist, deformation mechanisms of both phases will operate, and the dominating mechanism would depend on the proportion of each phase which is further determined by the testing temperature as well as the applied load. Since the testing temperature is very close to $A_f$ temperature (92 °C), we would expect that the majority of the microstructure is austenite phase with a small amount of martensite. Hence, during wear tests, deformation of both martensite and austenite will take place, while the deformation mechanism of austenite will dominate the contact area.

When tested at 90 °C, under low applied load at which the contact stress is below the stress-plateau of austenite (320 MPa at 90 °C), the austenite will be deformed elastically. Meanwhile, the martensite will be further deformed and detwinning will occur since the critical stress for detwinning is much lower than that of the SIMT. However, due to the presence of the small amount of martensite, the plastic strain accumulation associated with martensite detwinning is insignificant in the present study. Therefore, the surface damage is insignificant. One example is shown in Fig. 2(a), when tested under 50 mN, insignificant damage had been observed while the coefficient of friction was maintained at a low value.

When the load is increased, SIMT will occur. Since the SIMT is not fully reversible at 90 °C ($<A_f$), a plastic strain can be accumulated in the repeated wearing cycles. At 90 °C under 100 and 200 mN, the coefficient of friction had decreased from around 0.8 to 0.4 and stabilized thereafter, while debris and tracks were observed after 1000 wear cycles. The transition wear was supported by the decrease-and-stabilization behavior of the coefficient of friction in the wear process. In the beginning of test, the coefficient of friction had increased quickly due to the plastic strain accumulation when high asperities on surfaces adapted to each other. Some martensite detwinning may also have occurred at this stage. Thereafter, the pseudoelastic deformation dominated the contact area and the coefficient of friction had decreased drastically due to the effective deformation strain accommodation. The contact stress has exceeded the stress-plateau but below the yield stress of stress-induced martensite.

When tested under 300 mN, the wear entered the abrasive wear stage since a large amount of debris was observed after a small number of wear cycles. The contact stress likely exceeded the yield stress of stress-induced martensite/detwinned martensite and the plastic deformation dominated the wear process. On the other hand, according to the Clausius–Clapeyron equation, the critical stress for SIMT increases with increasing temperature.[27,28] Hence, a larger amount of plastic strain will be accumulated at 90 °C than that at 120 °C. This is in consistence with the observations where better wear resistance had been observed at 120 °C.

The effect of temperature on the wear behavior of NiTi SMA is summarized in Fig. 6. Three temperature regimes corresponding to different microstructures were classified, and the dominating deformation mechanisms were schematically illustrated under each regime. The coefficient of friction at 100th and 1000th wear cycles was compared to further verify the deformation mechanisms proposed.

When the $T < M_f$, the near-zero wear stage has been dominated by reversible elastic deformation of twinned martensite, leading to insignificant plastic strain accumulation, hence insignificant wear on surface. In the transition wear stage, the stabilized wear process has been dominated by the detwinning process. Due to the deformation strain accommodation in the detwinning process, wear on surface has been reduced. Moreover, plastic deformation has dominated the abrasive wear stage at higher loads, and severe damage was introduced within 100 wear cycles.

When $M_f < T < A_f$, in the near-zero wear stage, the majority of austenite has been deformed elastically, which is fully reversible thus introduced insignificant plastic strain. Meanwhile, the small portion of martensite was detwinned and caused insignificant plastic strain accumulation. However, the proportion of each phase will affect the wear behavior since martensite and austenite have difference yield stresses and martensite

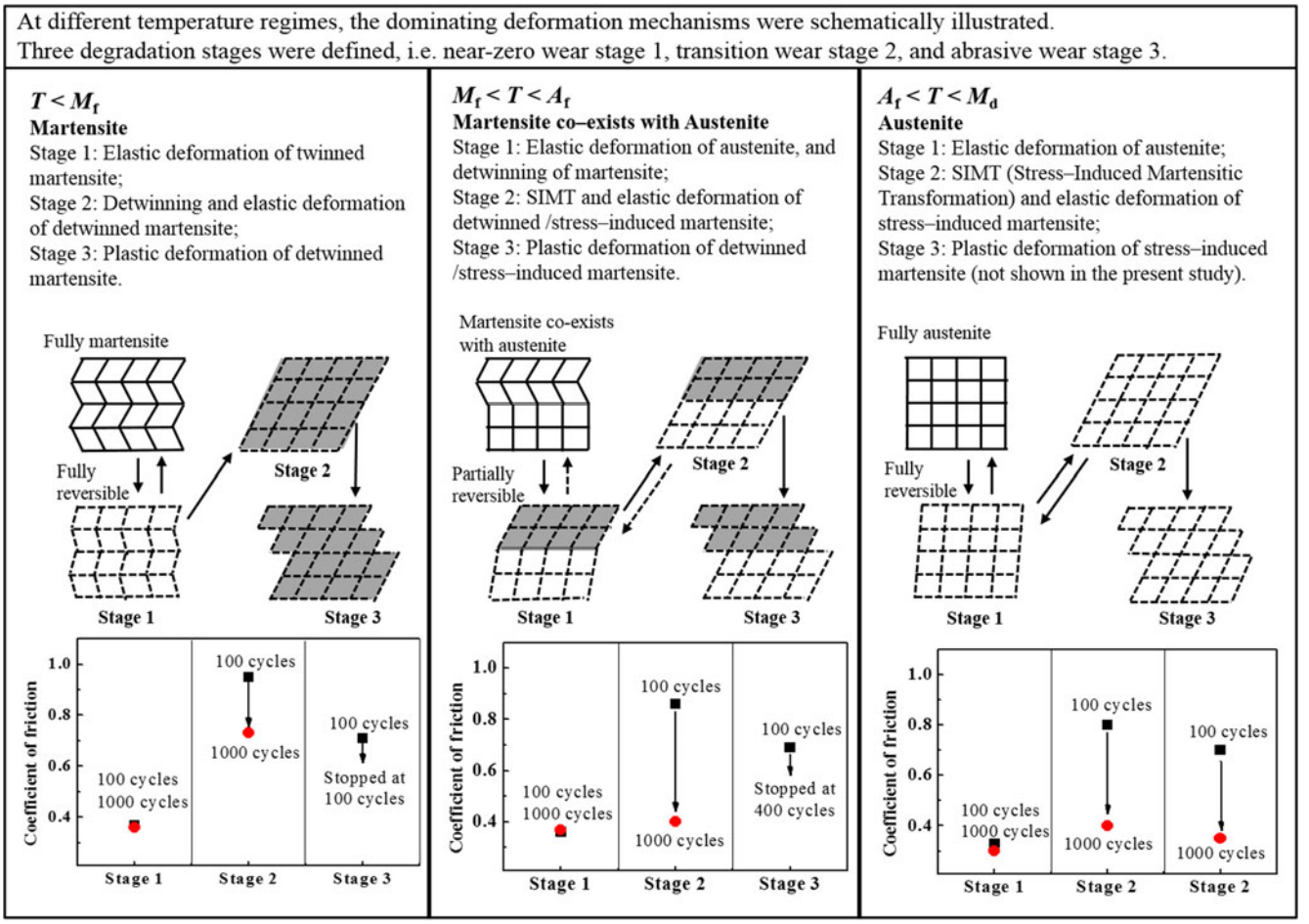


FIG. 6. Summary of the effect of the temperature on the wear behavior of NiTi SMA (the detwinned martensite was indicated by gray color to differentiate with stress-induced martensite).

detwinning is irrecoverable at constant temperature. For the ease of illustration, an equal percentage of martensite and austenite is shown in Fig. 6. In the transition wear stage, the SIMT has dominated the stabilized wear process. The effective deformation strain accommodation due to a SIMT process has significantly reduced wear. Furthermore, the abrasive wear stage behaved similarly to that tested below $M_f$, which has been attributed to the similar plastic deformation that dominated the wear process.

When $T > A_f$, the elastic deformation of austenite has dominated the near-zero wear process. Due to the increased temperature, hence increased critical stress for SIMT, more deformation strain has been accommodated. As a result, the plastic deformation of austenite phase was suppressed, hence the wear resistance was improved. When the applied load was further increased, in the run-in period, the plastic strain has accumulated and followed by a transition to the stabilized wear process dominated by SIMT, accompanying by less plastic strain accumulation in further wear cycles.

## V. CONCLUSIONS

The wear behavior of NiTi SMA was found closely related to the testing temperature due to the presence of different microstructures:

(1) When below $M_f$, the coefficient of friction had decreased from about 1.0 to 0.8 and thereafter stabilized at a lower value with further increasing wear cycles. Transition wear occurred and different wear mechanisms were involved as a function of wear cycles. The initial wear process is dominated by the plastic deformation of high asperities existing on the surfaces, whereas after transition, the martensite detwinning process dominated the wear.

(2) When tested above $M_f$ but below $A_f$, the coefficient of friction had decreased from around 0.8 to 0.4 associated with a transition to stabilization. Since martensite coexisted with austenite at this temperature, the SIMT of austenite has contributed to the wear resistance which was more effective in resisting wear as compared with that tested below $M_f$. Within this temperature range, the overall wear resistance of the material depends on the proportion of each phase, being that the austenite phase is

more wear resistant than that of martensite due to SIMT with higher yield stress and larger recoverable strain at constant temperature.

(3) When tested above $A_f$, the material is in fully austenitic state and the coefficient of friction had decreased from about 0.8 to 0.4 followed by a stabilization at lower value. Due to increased yield stress at increased temperature, the material shows improved wear resistance even under higher load. Therefore, the surface degradation process has been retarded at above $A_f$, and the fully reversible SIMT with increased yield stress was suggested as the main contributing factor in resisting wear.

## ACKNOWLEDGMENT

L. Yan is grateful for the research scholarship provided by Nanyang Technological University.

## REFERENCES

1. R. Sachdeva and S. Miyazaki: Application of shape memory nickel–titanium alloys to orthodontics. *Proc. Int. Mtg. Adv. Mater.* **9**, 605 (1988).
2. J.D. Harrison and D.E. Hodgon: *Shape Memory Effect in Alloys* (Plenum Publisher, New York, 1975).
3. J. Jin and H. Wang: Wear resistance of Ni–Ti alloy. *Acta Metall. Mater.* **24**, 66 (1988).
4. D.Y. Li and R. Liu: The mechanism responsible for high wear resistance of pseudo-elastic TiNi alloy – a novel tribo-material. *Wear* **225–229**, 777 (1999).
5. V. Imbeni, C. Martini, D. Prandstraller, G. Poli, C. Trepanier, and T.W. Duerig: Preliminary study of micro-scale abrasive wear of a NiTi shape memory alloy. *Wear* **254**, 1299 (2003).
6. P. Clayton: Tribological behavior of a titanium–nickel alloy. *Wear* **162–164**, 202 (1993).
7. D.Y. Li: Wear behavior of TiNi shape memory alloys. *Scr. Mater.* **34**, 195 (1996).
8. M. Abedini, H.M. Ghasemi, and M.N. Ahmadabadi: Tribological behavior of NiTi alloy in martensitic and austenitic states. *Mater. Des.* **30**, 4493 (2009).
9. R. Liu, D.Y. Li, Y.S. Xie, R. Llewellyn, and H.M. Hawthorne: Indentation behavior of pseudoelastic TiNi alloy. *Scr. Mater.* **41**, 691 (1999).
10. Y.N. Liang, S.Z. Li, Y.B. Jin, W. Jin, and S. Li: Wear behavior of a TiNi alloy. *Wear* **198**, 236 (1996).
11. L.M. Qian, Q.P. Sun, and X.D. Xiao: Role of phase transition in the unusual microwear behavior of superelastic NiTi shape memory alloy. *Wear* **260**, 509 (2006).
12. M. Arciniegas, J. Casals, J.M. Manero, J. Peña, and F.J. Gil: Study of hardness and wear behavior of NiTi shape memory alloys. *J. Alloys Compd.* **460**, 213 (2008).
13. X.Q. Feng, L.M. Qian, W.Y. Yan, and Q.P. Sun: Wearless scratch on NiTi shape memory alloy due to phase transformational shakedown. *Appl. Phys. Lett.* **92**, 121909 (2008).
14. D.Y. Li: Exploration of TiNi shape memory alloy for potential application in a new area: Tribological engineering. *Smart Mater. Struct.* **9**, 717 (2000).
15. S. Gialanella, G. Ischia, and G. Straffelini: Phase composition and wear behavior of NiTi alloys. *J. Mater. Sci.* **43**, 1701 (2008).
16. G.S. Firstov, R.G. Vitchev, H. Kumar, B. Blanpain, and J. Van Humbeeck. Surface oxidation of NiTi shape memory alloy. *Biomaterials* **23**, 4863 (2002).
17. K.L. Johnson: *Contact Mechanics* (Cambridge University Press, Cambridge, 1985).
18. D.C. Lagoudas: *Shape Memory Alloys: Modeling and Engineering Applications* (Springer, Texas, 2008).
19. Y. Liu, Z.L. Xie, J. Van Humbeeck, and L. Delaey: Asymmetry of stress–strain curves under tension and compression for NiTi shape memory alloys. *Acta Mater.* **46**, 4325 (1998).
20. L. Yan, Y. Liu, and E. Liu: Wear behavior of martensitic NiTi shape memory alloy under ball-on-disk sliding tests. *Tribol. Int.* **66**, 219 (2013).
21. L.M. Qian, Q.P. Sun, and Z. Zhou: The role of martensite reorientation in the fretting behavior of nickel titanium shape memory alloy. *Proc. Inst. Mech. Eng.* **222**, 887 (2008).
22. K. Otsuka and X. Ren: Physical metallurgy of Ti–Ni–based shape memory alloys. *Prog. Mater. Sci.* **50**, 511 (2005).
23. Z.L. Xie, Y. Liu, and J. Van Humbeeck: Microstructure of NiTi shape memory alloy due to tension–compression cyclic deformation. *Acta Mater.* **46**, 1989 (1998).
24. L. Orgeas and D. Favier: Stress-induced martensitic transformation of a NiTi alloy in isothermal shear, tension and compression. *Acta Mater.* **46**, 5579 (1998).
25. R. Plietsch and K. Ehrlich: Strength differential effect in pseudoelastic NiTi shape memory alloys. *Acta Mater.* **45**, 2417 (1997).
26. A.L. McKelvey and R.O. Ritchie: On the temperature dependence of the superelastic strength and the prediction of the theoretical uniaxial transformation strain in Nitinol. *Philos. Mag. A* **80**, 1759 (2000).
27. A.J. Muir Wood and T.W. Clyne: Measurement and modeling of the nanoindentation response of shape memory alloys. *Acta Mater.* **54**, 5607 (2006).
28. K. Otsuka and K. Shimize: Pseudoelasticity and shape memory effects in alloys. *Int. Met. Rev.* **31**, 93 (1986).